Emergent math xmlns="http://www.w3.org/1998/Math/MathML" display="inline">mrow>msub>mrow>mi mathvariant="double-struck">Z/mi>/mrow>mrow> mn>2/mn>/mrow>/msub>/mrow>/math> Gauge Theories and Topological Excitations in Rydberg Atom Arrays

Rhine Samajdar, Darshan G. Joshi, Yanting Teng, and Subir Sachdev

Phys. Rev. Lett. **130**, 043601 — Published 23 January 2023

DOI: 10.1103/PhysRevLett.130.043601

Emergent $\mathbb{Z}_2$ gauge theories and topological excitations in Rydberg atom arrays

Rhine Samajdar,[1] Darshan G. Joshi,[1] Yanting Teng,[1] and Subir Sachdev[1,2]

[1] *Department of Physics, Harvard University, Cambridge, MA 02138, USA*
[2] *School of Natural Sciences, Institute for Advanced Study, Princeton, NJ 08540, USA*

Strongly interacting arrays of Rydberg atoms provide versatile platforms for exploring exotic many-body phases and dynamics of correlated quantum systems. Motivated by recent experimental advances, we show that the combination of Rydberg interactions and appropriate lattice geometries naturally leads to emergent $\mathbb{Z}_2$ gauge theories endowed with matter fields. Based on this mapping, we describe how Rydberg platforms could realize two distinct classes of topological $\mathbb{Z}_2$ quantum spin liquids, which differ in their patterns of translational symmetry fractionalization. We also discuss the natures of the fractionalized excitations of these $\mathbb{Z}_2$ spin liquid states using both fermionic and bosonic parton theories and illustrate their rich interplay with proximate solid phases.

Programmable arrays of Rydberg atoms [1–4] have recently emerged as powerful quantum simulators to probe important questions in diverse areas of physics. Over the years, these systems have been used as clean, tunable platforms to study interesting many-body phases [5, 6], quantum dynamics [7, 8], combinatorial optimization problems [9], and gauge theories [10–12].

Generically, the setup consists of atoms individually trapped in an array of optical tweezers and pumped by lasers to highly excited Rydberg states. The interaction between two atoms in the Rydberg state is very large at short distances, and this significant energy cost prohibits—or *blockades*—the simultaneous excitation of neighboring atoms, thereby inducing robust quantum correlations between the atomic states. This "Rydberg blockade" effect [13] can be exploited to study a number of interesting phases of quantum matter and the transitions between them, thus prompting a wealth of experimental [5, 14–17] and theoretical [18–26] investigation.

Quantum spin liquids (QSLs) form one such class of highly sought-after phases of matter. These are strongly correlated phases characterized by long-range many-body quantum entanglement, which gives rise to exotic properties such as fractionalized excitations, emergent gauge fields, and topological ground-state degeneracies [27–29]. The simplest example of such a QSL which does not break any symmetries, including time-reversal, is the $\mathbb{Z}_2$ spin liquid [30–32]—a stable, gapped quantum state with the same topological order as the toric code [33]. Despite some indications that such a phase may exist in certain electronic systems on the kagome lattice [34], direct experimental detection thereof has so far proved elusive in solid-state materials.

Today, efforts towards realizing $\mathbb{Z}_2$ QSL phases have turned to Rydberg atom arrays. A promising playground to look for QSL phases is the family of quantum dimer models [35, 36]. Recently, Ref. 37 theoretically showed that the phases of various quantum dimer models [35, 36] can be efficiently implemented using Rydberg atoms arrayed on the *sites* of a kagome lattice and argued that Rydberg platforms could be used to realize topological spin liquid states based solely on their native interactions [38]. Recent experiments on an array of Rydberg atoms placed on the *links* of a kagome lattice yielded evidence for a state with topological correlations [6], in accordance with theoretical proposals [39]. However, even though numerics and experiments support a $\mathbb{Z}_2$ QSL phase, a general understanding of the connection between Rydberg atom arrays and $\mathbb{Z}_2$ QSLs remains to be obtained.

In this Letter, we bridge the gap and establish the underlying reason *why* geometrically frustrated Rydberg atom arrays host spin liquids. We do so by constructing an *exact* mapping from the Rydberg Hamiltonian to a $\mathbb{Z}_2$ gauge theory. In this formulation, the $\mathbb{Z}_2$ QSL is nothing but the deconfined phase of the gauge theory while the various ordered solids correspond to the confined phases. However, this emergent gauge theory is necessarily endowed with matter fields. These matter fields are the three distinct anyonic quasiparticle excitations of the $\mathbb{Z}_2$ QSL. Such fractional excitations are the hallmark of a QSL, and can be either bosonic (e and m) or fermionic (ε). The e and ε anyons are particle-like excitations, and are collectively referred to as "spinons", whereas the m anyon is a vortex-like excitation called a "vison" [40]. For each of these excitations, constructing detailed parton theories (which are widely employed effective theories for anyonic excitations of QSLs [27, 30, 41]), we analyze their static spectra using fully self-consistent mean-field theory and illustrate their relation to neighboring non-topological phases in the context of spinon condensation.

Importantly, depending on whether elementary translations anticommute or commute when acting on the visons, $\mathbb{Z}_2$ spin liquids can be further classified as "odd" or "even", respectively [42–44]. We highlight how this subtle distinction is reflected in a parton formulation and adds to the rich variety of possible QSL states.

Model.—In the simplest description, each Rydberg atom can be effectively regarded as a two-level system (i.e., a qubit). We identify the atomic ground state $|g\rangle$ with an empty bosonic state $|0\rangle$ and the Rydberg state $|r\rangle$ with the filled bosonic state $B^\dagger|0\rangle$ (Fig. 1). By construction, this mapping associates the states with "hard-core" bosons, i.e., $N_\ell \equiv B_\ell^\dagger B_\ell = 0, 1$. These two states are coupled by the external lasers with a Rabi frequency Ω. The

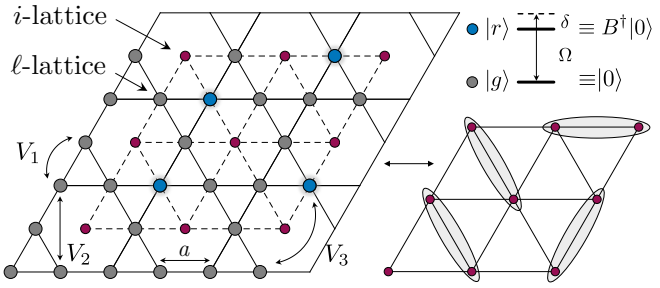

Figure 1. Rydberg atoms are positioned on the sites of the kagome ℓ-lattice with lattice spacing a; the associated i-lattice (red dots) is triangular. The two atomic states $|g\rangle$ and $|r\rangle$ are depicted in gray and blue, respectively. Here, V_p represents the interaction between p-th-nearest neighbors. [Upper-right]: The effective two-level bosonic mode defined by the presence, $B^\dagger|0\rangle$, or absence, $|0\rangle$, of the Rydberg excitation. [Lower-right]: Mapping of the configuration shown on the left to the triangular-lattice dimer model, where an occupied boson (blue circle) on the kagome lattice is mapped to the presence of a dimer on the link of the triangular lattice. In general, any configuration of Rydberg excitations can be mapped to a set of dimers that need not satisfy a close-packing constraint.

frequency of the laser is adjusted such that the detuning away from resonance of the $|g\rangle$ to $|r\rangle$ transition is δ (see Fig. 1). Atoms in the Rydberg state interact via a van der Waals potential of the form $\mathcal{V}(\boldsymbol{r}) \equiv V_0/r^6$, which arises from strong dipole-dipole interactions. Putting these ingredients together, the full Hamiltonian [45, 46] is given by

$$H_{\text{FSS}} = \sum_\ell \left[\frac{\Omega}{2}\left(B_\ell + B_\ell^\dagger\right) - \delta N_\ell\right] + \frac{1}{2}\sum_{\ell\neq\ell'} V_{\ell,\ell'} N_\ell N_{\ell'}, \tag{1}$$

where ℓ labels a set points on the kagome lattice with position $\boldsymbol{r}_\ell$ and we have defined $V_{\ell,\ell'} \equiv \mathcal{V}(\boldsymbol{r}_\ell - \boldsymbol{r}_{\ell'})$ for notational brevity. The interaction strength can equivalently be parametrized by the Rydberg blockade radius $R_b \equiv (V_0/\Omega)^{1/6}$; intuitively, this means that atoms within a radius of approximately R_b are blockaded from occupying the Rydberg state simultaneously. The first term in the Hamiltonian (1) breaks U(1) symmetry, so the number of B bosons is not conserved.

Emergent gauge theory.—At the moment, H_{FSS} is not a lattice gauge theory, and B_ℓ is the annihilation operator of a boson which does not carry gauge charges. We are interested here in configurations of the FSS model which can realize a $\mathbb{Z}_2$ spin liquid. To begin, we identify the two bosonic states on each site with the qubits of a $\mathbb{Z}_2$ gauge theory as $B_\ell + B_\ell^\dagger = \sigma_\ell^z$, $N_\ell = (1-\sigma_\ell^x)/2$. Then, without approximation, one can write the FSS model as a model of interacting qubits:

$$H_{\text{FSS}} = \frac{1}{2}\sum_\ell \left[\Omega\,\sigma_\ell^z + \delta\,\sigma_\ell^x\right] + \frac{1}{2}\sum_{\ell\neq\ell'} \frac{V_{\ell,\ell'}}{4}(1-\sigma_\ell^x)(1-\sigma_{\ell'}^x)\,. \tag{2}$$

In order to study possible $\mathbb{Z}_2$ spin liquid states, we explore making (2) gauge invariant by introducing zero-energy matter fields which carry a $\mathbb{Z}_2$ gauge charge. First, we introduce an "i-lattice" of sites $i, j, \ldots$, such that the centers of the (i, j) links on the i-lattice coincide with the ℓ sites in Eq. (2) (see Figure 1). Note that the i-lattice has to be defined in a manner which does not break any symmetries of the ℓ-lattice. Such a construction is feasible for only some lattices—like the kagome [37] and the ruby [39]—but not others; e.g., the square and honeycomb ℓ-lattices do not have a corresponding i-lattice.

The i-lattice qubits are acted on by Pauli matrices $\tau_i^{x,y,z}$, and these transform under $\mathbb{Z}_2$ lattice gauge transformations as $\sigma_{\bar{i}\bar{j}}^z \to \varrho_i \sigma_{\bar{i}\bar{j}}^z \varrho_j$, $\sigma_{\bar{i}\bar{j}}^x \to \sigma_{\bar{i}\bar{j}}^x$, $\tau_i^z \to \tau_i^z \varrho_i$, $\tau_i^x \to \tau_i^x$, with $\varrho_i = \pm 1$, where $\sigma_{\bar{i}\bar{j}}^z \equiv \sigma_\ell^z$ on the ℓ-lattice site between the i and j sites on the i-lattice. Then, an explicitly $\mathbb{Z}_2$-gauge-invariant form of the FSS Hamiltonian is

$$\mathcal{H}_{\text{FSS}} = \frac{\Omega}{2}\sum_{\langle\bar{i}\bar{j}\rangle} \tau_i^z \sigma_{\bar{i}\bar{j}}^z \tau_j^z + \frac{\delta}{2}\sum_\ell \sigma_\ell^x + \sum_{\ell\neq\ell'} \frac{V_{\ell,\ell'}}{8}(1-\sigma_\ell^x)(1-\sigma_{\ell'}^x). \tag{3}$$

The other canonical terms of Ising gauge theory, which are unessential to our discussion here, are described in Sec. SI of the Supplemental Material (SM) [47].

With the introduction of the τ^z Ising matter fields, we also introduce an infinite number of gauge charges G_i that commute with $\mathcal{H}_{\text{FSS}}$ as $G_i = \tau_i^x \prod_{\ell \text{ ends on } i} \sigma_\ell^x$, $[\mathcal{H}_{\text{FSS}}, G_i] = 0$; we choose $G_i = 1$, whereupon the Hilbert space of Eq. (3) is identical to that of Eq. (1). In the $\mathbb{Z}_2$ gauge theory framework, there is a unit $\mathbb{Z}_2$ electric charge on each lattice site of an odd $\mathbb{Z}_2$ gauge theory, which is a manifestation of nontrivial lattice symmetry fractionalization in this phase [48–51]. The visons see the spinons as a source of π flux, so the adiabatic motion of a vison around a lattice site picks up a phase of $+1\,(-1)$ in an even (odd) QSL. Thus, without dynamic matter, a state with $\tau_i^x = 1\,(-1)\,\forall\, i$ will correspond to an even (odd) $\mathbb{Z}_2$ spin liquid; with dynamic matter, these identifications will continue to hold in a phase where τ_i^x has small fluctuations from the matter-free case.

Mean-field theory of bosonic spinons.—Focusing hereafter on the case where the ℓ-lattice is the kagome and the i-lattice is triangular (Fig. 1), we formulate a theory for the ground state and its e excitations by returning to the bosonic description in Eq. (1). The $\tau_i^{x,z}$ operators can be similarly represented in terms of hard-core bosons b such that $b_i + b_i^\dagger = \tau_i^z$, $b_i^\dagger b_i \equiv n_i = (1 \pm \tau_i^x)/2$, where the signs correspond to the odd/even cases, so that $\langle n_i \rangle \ll 1$ for both. Then, the gauge charge operator can be rewritten as $G_i = \exp\left(i\pi\left[\tilde{n}_i + \sum_{\ell \text{ ends on } i} N_\ell\right]\right)$, where $\tilde{n}_i \equiv n_i\,(\equiv n_i + 1)$ for an even (odd) QSL; so, we look for ground states with $n_i + \sum_{\ell \text{ ends on } i} N_\ell = 1, 2$. We can now perform a self-consistent mean-field theory calculation, after expressing Eq. (3) in terms of B_ℓ and b_i, and imposing the constraint above by a Lagrange multiplier.

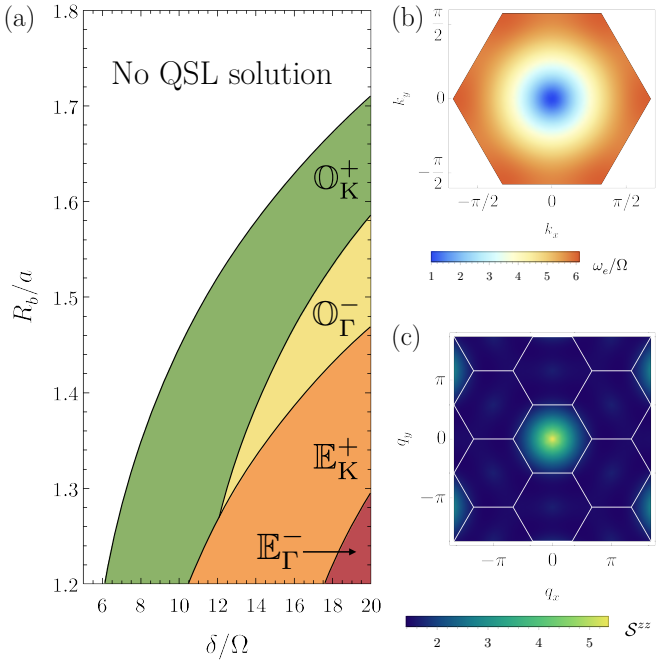

Figure 2. (a) Mean-field phase diagram highlighting the four possible QSL solutions for e-spinons. Corrections beyond mean-field are expected to shift the QSL phases' boundaries towards smaller δ/Ω and larger R_b/a. Note that the extent of the nematic solid in the DMRG phase diagram of Ref. 37 is set by the points where the visons of the QSLs condense. There are four distinct types of QSL solutions which we label as $[\mathbb{E}/\mathbb{O}]^{[+/-]}_{[\mathrm{K}/\Gamma]}$, based on the even (odd) nature of the QSL and the location of the spinon dispersion minimum. (b) Representative energy dispersion of the bosonic spinon excitation of the $\mathbb{O}_{\Gamma}^{-}$ QSL in the first Brillouin zone. (c) The static structure factor of this state (calculated from the e particle theory) displays prominent spectral weight at the Γ point but is broadly featureless in the extended Brillouin zone (cf. Fig. S2).

In this process [47], we condense B_ℓ and replace it with a real number $\mathcal{B}$. Retaining terms quadratic in b_i and diagonalizing the resulting Bogoliubov Hamiltonian, we arrive at the gapped e-particle spectrum. We note that such a diagonalization procedure via a Lagrange multiplier only imposes the Gauss-law constraint on average (see SM, Sec. SII [47]).

The results of such an analysis are presented in Fig. 2 and Figs. S1–S3 [47]. In total, we find four distinct nontrivial QSL states, which we label as $[\mathbb{E}/\mathbb{O}]^{[+/-]}_{[\mathrm{K}/\Gamma]}$. In this notation, $\mathbb{E}$ and $\mathbb{O}$ denote even and odd spin liquids, respectively, the $\pm$ in the superscript indicates the sign of $\mathcal{B}$ in the corresponding solution, and the subscript conveys whether the minima of the dispersion in the Brillouin zone occur at the Γ point or at the K, K$'$ points. In Fig. 2(a), we construct a mean-field phase diagram by plotting the lowest-energy solution among these four at each point in parameter space. While mean-field theory is not expected to capture the precise parameter values for QSL solutions, it does correctly describe the change in the nature of the QSL state from even to odd as the density of Rydberg excitations decreases with increasing R_b/a [38].

The representative spectra of the candidate Rydberg QSLs are shown in Fig. 2(b) and Fig. S2(a–c) [47]. While all these states are gapped, one can reach an instability of the QSL state by tuning some parameter to bring the quasiparticle energy gap to zero. Then, the transition *out* of the QSL into the proximate phases can be viewed as a condensation of the bosonic spinon [32, 52]. For instance, consider the $\mathbb{O}_{\Gamma}^{-}$ QSL [Fig. 2(b)]: since its dispersion minimum occurs at the Γ point, when the b_i are also condensed, one obtains a trivial paramagnetic or "disordered" phase as is commonly observed in the Rydberg phase diagram [37]. This quantum phase transition [53] belongs to the so-called Ising* universality class [54–56]. Moreover, to investigate spin correlations in the QSL phase, in Figs. 2(c) and S2, we analytically calculate the static structure factor $\mathcal{S}^{zz}(\boldsymbol{q}) = \sum_{\ell_1,\ell_2} e^{i\boldsymbol{q}\cdot(\boldsymbol{r}_{\ell_1}-\boldsymbol{r}_{\ell_2})} \langle \sigma^z_{\ell_1}\sigma^z_{\ell_2}\rangle / \mathcal{N}_\ell$ [Eq. (S24) in the SM] in Fourier space based on the two-point functions $\langle \sigma^z_{\ell_1}\sigma^z_{\ell_2}\rangle$. Such correlation function can be measured via implementation of local basis-rotation operations detailed, for instance, in Ref. 6. Since it only requires measurement of local observables, $\mathcal{S}^{zz}$ provides a nontrivial experimentally accessible prediction to probe and distinguish possible spin liquid states.

Pictorially, the Ising electric charge e, which sits at the center of the hexagonal plaquettes of the kagome lattice, is defined by "defect hexagons" [57] such that $\prod_{\ell\in\hexagon}\sigma^x_\ell = -1\,(+1)$ for an even (odd) QSL, as sketched in Fig. 3(a). It is also easy to see from this figure why the gauge-charged matter fields τ^x are gapped. Naively, given the presence of τ^z-gapless matter, one could anticipate that τ^z would condense, destroying any possible $\mathbb{Z}_2$ QSL phase. However, from Fig. 3(a), we notice that the motion of the Ising matter τ^x requires a σ^z operation; by virtue of the qubit–boson mapping, this can add or remove a B_ℓ boson, leading to a large energetic cost from either $V(\mathbf{r})$ or δ, respectively. Consequently, τ^x gauge charge fluctuations are expensive, and this could help stabilize a deconfined phase of the $\mathbb{Z}_2$ gauge theory (3).

Dual theory of visons.—The second type of bosonic excitations of the $\mathbb{Z}_2$ QSL are the visons, which carry $\mathbb{Z}_2$ magnetic flux [40, 58]. For a full description of the m particles, we perform a duality transformation on Eq. (3) to obtain an Ising gauge theory with Ising matter on the lattice dual to the (triangular) i-lattice. This is the medial *honeycomb* lattice formed by connecting the centers of the kagome triangles [Fig. 3(b)]; on its sites, we define the Ising matter fields $\mu^z_{i'} = \pm 1$, and on its links, we introduce the gauge fields $\eta^z_{i'j'} = \pm 1$. The mapping between the direct (σ,τ) and dual (η,μ) variables is derived in Sec. SIIIA [47], following which, we arrive at the theory

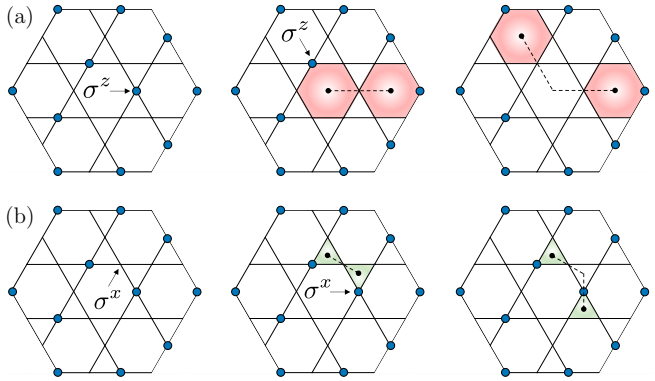

Figure 3. (a) Creation and motion of bosonic spinon (e particle) excitations in an even QSL by the repeated application of σ^z, as depicted from left to right. The red plaquettes identify the defect hexagons on which the spinons reside. (b) Same, but for the visons (m particles), which live at the centers of the kagome triangles. Both excitations can only be created in pairs by any local operator acting on the ground state.

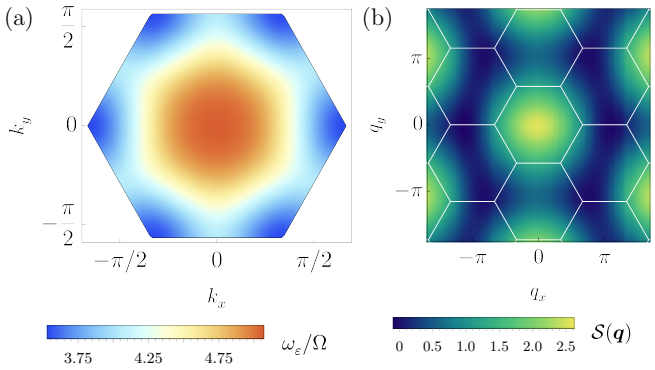

Figure 4. (a) Mean-field spectrum of the ε particle and (b) the resultant static structure factor at $\delta/\Omega = 4.0$, $R_b/a = 1.6$. The qualitative nature of the fermionic band structure and static structure factor is the same for all $(\delta/\Omega,\ R_b/a)$ for which a QSL solution is found.

for the visons:

$$\tilde{\mathcal{H}}_{\text{FSS}} = \frac{\Omega}{2}\sum_{\langle \bar{i}'\bar{j}'\rangle}\eta^x_{\bar{i}'\bar{j}'} + \frac{\delta}{2}\sum_{\langle \bar{i}'\bar{j}'\rangle}\left(\mu^z_{\bar{i}'}\eta^z_{\bar{i}'\bar{j}'}\mu^z_{\bar{j}'} - 1\right) \tag{4}$$
$$+ \sum_{\langle \bar{i}'\bar{j}'\rangle\neq\langle \bar{k}'\bar{l}'\rangle}\frac{V(\boldsymbol{r}_{\bar{i}'\bar{j}'} - \boldsymbol{r}_{\bar{k}'\bar{l}'})}{8}\left(1-\mu^z_{\bar{i}'}\eta^z_{\bar{i}'\bar{j}'}\mu^z_{\bar{j}'}\right)\left(1-\mu^z_{\bar{k}'}\eta^z_{\bar{k}'\bar{l}'}\mu^z_{\bar{l}'}\right).$$

Upon restricting ourselves to only nearest-neighbor blockade interactions for simplicity and with the appropriate choice of a gauge (in the limit of low spinon densities), the minimal theory of the visons reduces to an Ising model on the honeycomb lattice [Eq. (S41)] with first- (J_1) and second-nearest-neighbor (J_2) Ising interactions (see Sec. SIIIB [47]). For the even QSL, Roychowdhury *et al.* [57] demonstrated that in the presence of a third-nearest-neighbor interaction J_3 (which would arise from the long-ranged Rydberg tails in our case), there is an extended regime in $J_{1,2,3}$ parameter space where the minima of the vison spectra occur at the three inequivalent M points in the Brillouin zone. Pairwise condensation of these visons would then describe the transition to a threefold-rotational-symmetry-breaking "nematic" phase of Rydberg atoms on the kagome lattice [37, 57], characterized by ordering wavevectors at $2\text{M}_{1,2,3}$. Furthermore, in Sec. SIIIB [47], we show that for the odd QSL, the minima of the vison dispersion are also consistent with the development of nematic order by vison condensation, but can additionally reproduce a subset of the ordering peaks of a proximate "staggered" phase [37, 57].

Fermionic spinons.—The anyon content of the $\mathbb{Z}_2$ QSL also includes a fermionic spinon. In order to obtain a theory of this ε particle, we use the Abrikosov fermion representation [59–61], in which the spin operator at each site is fractionalized as $\vec{S}_\ell \equiv \vec{\sigma}_\ell/2 = (f^\dagger_\ell\,\vec{\rho}\,f_\ell)/2$, with $f_\ell \equiv (f_{\ell,1}, f_{\ell,2})^{\text{T}}$ being a two-component fermionic spinon operator, and $\vec{\rho}$ denoting the three Pauli matrices.

Writing H_{FSS} in terms of these fermionic spinons generates four-fermion terms, which we decouple into fermion bilinears by introducing the mean-field parameters $t^{\alpha\beta}_{\ell,\ell'} \equiv \langle f^\dagger_{\ell,\alpha} f_{\ell',\beta}\rangle$, $\Delta^{\alpha\beta}_{\ell,\ell'} \equiv \langle f_{\ell,\alpha} f_{\ell',\beta}\rangle$. The expectation values $\{t^{\alpha\beta}_{\ell,\ell'}, \Delta^{\alpha\beta}_{\ell,\ell'}\}$ then collectively define a mean-field *ansatz*. The projective action [41, 48] of lattice or time-reversal symmetries on this ansatz describes the particular QSL state of interest. Unlike systems with SU(2) spin-rotation symmetry (for which $\langle f^\dagger_{i,\alpha} f_{j,\beta}\rangle \propto \delta_{\alpha\beta}$ and $\langle f_{i,\alpha} f_{j,\beta}\rangle \propto \epsilon_{\alpha\beta}$ [62]), in our ansatz, we have to allow for hopping and pairing terms with all possible combinations of α, β due to the lack of spin-rotation invariance in Eq. (2). The full theory thus obtained is detailed in Sec. SIV of the SM [47] [see Eq. (S66)]. Self-consistently solving for $\{t^{\alpha\beta}_{\ell,\ell'}, \Delta^{\alpha\beta}_{\ell,\ell'}\}$ then yields the fermionic band structure. As illustrated in Fig. 4(a), we observe that the ε particle is gapped too and the minima of its dispersion occur at the K, K' points. To determine the experimental signatures of this QSL state, we also calculate its static structure factor in Fig. 4(b) and find that it has broad features located at $\boldsymbol{q} = \Gamma$ but no sharp Bragg peaks anywhere in the extended Brillouin zone, indicating the absence of long-range order. The distribution of the spectral weight in $\mathcal{S}(\boldsymbol{q})$ resembles that of the bosonic theory's structure factor in Fig. 2(c), but is notably distinct from the other candidates sketched in Fig. S2(a,c).

Discussion and outlook.—In this work, we have shown how systems of Rydberg atoms arrayed on kagome or ruby lattices can give rise to emergent $\mathbb{Z}_2$ gauge theories with matter fields; the deconfined phase of such a gauge theory is a $\mathbb{Z}_2$ quantum spin liquid. We develop a formalism to systematically characterize all three classes of topological excitations of this $\mathbb{Z}_2$ QSL, evaluate their spectral properties in a parton description [Eqs. (3), (4), and (S66)], and discuss their experimental fingerprints in static structure factors. In particular, we identify a

promising QSL candidate, labeled $\mathbb{O}_\Gamma^-$, which is consistent with observations of neighboring nematic and disordered phases in the framework of vison/spinon condensation [37]. These results bear direct relevance to recent and ongoing experiments on Rydberg quantum simulators that have opened the door to realizing and probing highly entangled $\mathbb{Z}_2$ QSL states. Our analysis herein of the quasiparticle spectra and gaps should help inform the feasibility of dynamical preparation of such QSL states via quasiadiabatic sweeps [6, 63, 64].

We thank Tom Banks, Yuan-Ming Lu, Mikhail D. Lukin, Zi Yang Meng, Sergej Moroz, and our coauthors in prior collaborations [6, 37, 38] for useful discussions. This work was supported by the U.S. Department of Energy under Grant DE-SC0019030. D.G.J. acknowledges support from the Leopoldina fellowship by the German National Academy of Sciences through Grant No. LPDS 2020-01.

[1] M. Endres, H. Bernien, A. Keesling, H. Levine, E. R. Anschuetz, A. Krajenbrink, C. Senko, V. Vuletić, M. Greiner, and M. D. Lukin, Science **354**, 1024 (2016).
[2] A. Browaeys and T. Lahaye, Nat. Phys. **16**, 132 (2020).
[3] M. Morgado and S. Whitlock, AVS Quantum Sci. **3**, 023501 (2021).
[4] D. Bluvstein, H. Levine, G. Semeghini, T. T. Wang, S. Ebadi, M. Kalinowski, A. Keesling, N. Maskara, H. Pichler, M. Greiner, V. Vuletic, and M. D. Lukin, Nature **604**, 451 (2022).
[5] S. Ebadi, T. T. Wang, H. Levine, A. Keesling, G. Semeghini, A. Omran, D. Bluvstein, R. Samajdar, H. Pichler, W. W. Ho, S. Choi, S. Sachdev, M. Greiner, V. Vuletić, and M. D. Lukin, Nature **595**, 227 (2021).
[6] G. Semeghini, H. Levine, A. Keesling, S. Ebadi, T. T. Wang, D. Bluvstein, R. Verresen, H. Pichler, M. Kalinowski, R. Samajdar, A. Omran, S. Sachdev, A. Vishwanath, M. Greiner, V. Vuletić, and M. D. Lukin, Science **374**, 1242 (2021).
[7] C. J. Turner, A. A. Michailidis, D. A. Abanin, M. Serbyn, and Z. Papić, Nature Phys. **14**, 745 (2018).
[8] D. Bluvstein, A. Omran, H. Levine, A. Keesling, G. Semeghini, S. Ebadi, T. T. Wang, A. A. Michailidis, N. Maskara, W. W. Ho, S. Choi, M. Serbyn, M. Greiner, V. Vuletić, and M. D. Lukin, Science **371**, 1355 (2021).
[9] S. Ebadi, A. Keesling, M. Cain, T. T. Wang, H. Levine, D. Bluvstein, G. Semeghini, A. Omran, J.-G. Liu, R. Samajdar, X.-Z. Luo, B. Nash, X. Gao, B. Barak, E. Farhi, S. Sachdev, N. Gemelke, L. Zhou, S. Choi, H. Pichler, S.-T. Wang, M. Greiner, V. Vuletic, and M. D. Lukin, Science **376**, 1209 (2022).
[10] A. Celi, B. Vermersch, O. Viyuela, H. Pichler, M. D. Lukin, and P. Zoller, Phys. Rev. X **10**, 021057 (2020).
[11] F. M. Surace, P. P. Mazza, G. Giudici, A. Lerose, A. Gambassi, and M. Dalmonte, Phys. Rev. X **10**, 021041 (2020).
[12] D. González-Cuadra, T. V. Zache, J. Carrasco, B. Kraus, and P. Zoller, arXiv preprint (2022), arXiv:2203.15541 [quant-ph].
[13] D. Jaksch, J. I. Cirac, P. Zoller, S. L. Rolston, R. Côté, and M. D. Lukin, Phys. Rev. Lett. **85**, 2208 (2000).
[14] H. Bernien, S. Schwartz, A. Keesling, H. Levine, A. Omran, H. Pichler, S. Choi, A. S. Zibrov, M. Endres, M. Greiner, V. Vuletić, and M. D. Lukin, Nature **551**, 579 (2017).
[15] S. de Léséleuc, V. Lienhard, P. Scholl, D. Barredo, S. Weber, N. Lang, H. P. Büchler, T. Lahaye, and A. Browaeys, Science **365**, 775 (2019).
[16] A. Keesling, A. Omran, H. Levine, H. Bernien, H. Pichler, S. Choi, R. Samajdar, S. Schwartz, P. Silvi, S. Sachdev, P. Zoller, M. Endres, M. Greiner, V. Vuletić, and M. D. Lukin, Nature **568**, 207 (2019).
[17] P. Scholl, M. Schuler, H. J. Williams, A. A. Eberharter, D. Barredo, K.-N. Schymik, V. Lienhard, L.-P. Henry, T. C. Lang, T. Lahaye, A. M. Läuchli, and A. Browaeys, Nature **595**, 233 (2021).
[18] R. Samajdar, S. Choi, H. Pichler, M. D. Lukin, and S. Sachdev, Phys. Rev. A **98**, 023614 (2018).
[19] S. Whitsitt, R. Samajdar, and S. Sachdev, Phys. Rev. B **98**, 205118 (2018).
[20] N. Chepiga and F. Mila, Phys. Rev. Lett. **122**, 017205 (2019).
[21] N. Chepiga and F. Mila, Nat. Commun. **12**, 1 (2021).
[22] R. Samajdar, W. W. Ho, H. Pichler, M. D. Lukin, and S. Sachdev, Phys. Rev. Lett. **124**, 103601 (2020).
[23] T. Felser, S. Notarnicola, and S. Montangero, Phys. Rev. Lett. **126**, 170603 (2021).
[24] M. Kalinowski, R. Samajdar, R. G. Melko, M. D. Lukin, S. Sachdev, and S. Choi, Phys. Rev. B **105**, 174417 (2022).
[25] C. Miles, R. Samajdar, S. Ebadi, T. T. Wang, H. Pichler, S. Sachdev, M. D. Lukin, M. Greiner, K. Q. Weinberger, and E.-A. Kim, arXiv:2112.10789 [quant-ph] (2021).
[26] M. J. O'Rourke and G. K.-L. Chan, arXiv:2201.03189 [cond-mat.str-el] (2022).
[27] L. Savary and L. Balents, Rep. Prog. Phys. **80**, 016502 (2016).
[28] J. Knolle and R. Moessner, Annu. Rev. Condens. Matter Phys. **10**, 451 (2019).
[29] C. Broholm, R. J. Cava, S. A. Kivelson, D. G. Nocera, M. R. Norman, and T. Senthil, Science **367**, eaay0668 (2020).
[30] N. Read and S. Sachdev, Phys. Rev. Lett. **66**, 1773 (1991).
[31] X. G. Wen, Phys. Rev. B **44**, 2664 (1991).
[32] S. Sachdev, Phys. Rev. B **45**, 12377 (1992).
[33] A. Kitaev, Ann. Phys. **321**, 2 (2006).
[34] P. A. Lee, Science **321**, 1306 (2008).
[35] D. S. Rokhsar and S. A. Kivelson, Phys. Rev. Lett. **61**, 2376 (1988).
[36] R. Moessner and K. S. Raman, in *Introduction to Frustrated Magnetism* (Springer, 2011) pp. 437–479.
[37] R. Samajdar, W. W. Ho, H. Pichler, M. D. Lukin, and S. Sachdev, Proc. Natl. Acad. Sci. U.S.A. **118**, e2015785118 (2021), 2011.12295.
[38] Z. Yan, R. Samajdar, Y.-C. Wang, S. Sachdev, and Z. Y. Meng, Nat. Commun. **13**, 5799 (2022).
[39] R. Verresen, M. D. Lukin, and A. Vishwanath, Phys. Rev. X **11**, 031005 (2021).
[40] T. Senthil and M. P. A. Fisher, Phys. Rev. B **62**, 7850 (2000).
[41] X.-G. Wen, Phys. Rev. B **65**, 165113 (2002).
[42] R. A. Jalabert and S. Sachdev, Phys. Rev. B **44**, 686

(1991).
[43] S. Sachdev and M. Vojta, J. Phys. Soc. Japan. Suppl. B **69**, 1 (2000).
[44] R. Moessner, S. L. Sondhi, and E. Fradkin, Phys. Rev. B **65**, 024504 (2002).
[45] P. Fendley, K. Sengupta, and S. Sachdev, Phys. Rev. B **69**, 075106 (2004).
[46] S. Sachdev, K. Sengupta, and S. M. Girvin, Phys. Rev. B **66**, 075128 (2002).
[47] See Supplemental Material, which includes Refs. 65–81, for more details on the mapping to Ising gauge theory as well as parton theories for the e, m, and ε particles.
[48] A. M. Essin and M. Hermele, Phys. Rev. B **87**, 104406 (2013).
[49] X. Chen, F. J. Burnell, A. Vishwanath, and L. Fidkowski, Phys. Rev. X **5**, 041013 (2015).
[50] N. Tarantino, N. H. Lindner, and L. Fidkowski, New J. Phys. **18**, 035006 (2016).
[51] M. Barkeshli, P. Bonderson, M. Cheng, and Z. Wang, Phys. Rev. B **100**, 115147 (2019).
[52] F. A. Bais and J. K. Slingerland, Phys. Rev. B **79**, 045316 (2009).
[53] S. Sachdev, *Quantum Phase Transitions* (Cambridge University Press, New York, 2011).
[54] A. V. Chubukov, T. Senthil, and S. Sachdev, Phys. Rev. Lett. **72**, 2089 (1994).
[55] M. Schuler, S. Whitsitt, L.-P. Henry, S. Sachdev, and A. M. Läuchli, Phys. Rev. Lett. **117**, 210401 (2016).
[56] S. Whitsitt and S. Sachdev, Phys. Rev. B **94**, 085134 (2016).
[57] K. Roychowdhury, S. Bhattacharjee, and F. Pollmann, Phys. Rev. B **92**, 075141 (2015).
[58] N. Read and B. Chakraborty, Phys. Rev. B **40**, 7133 (1989).
[59] A. A. Abrikosov, Physics Physique Fizika **2**, 5 (1965).
[60] I. Affleck, Z. Zou, T. Hsu, and P. W. Anderson, Phys. Rev. B **38**, 745 (1988).
[61] J. B. Marston and I. Affleck, Phys. Rev. B **39**, 11538 (1989).
[62] Y.-M. Lu, Y. Ran, and P. A. Lee, Phys. Rev. B **83**, 224413 (2011).
[63] Y. Cheng, C. Li, and H. Zhai, arXiv preprint (2021), arXiv:2112.13688 [cond-mat.quant-gas].
[64] G. Giudici, M. D. Lukin, and H. Pichler, Phys. Rev. Lett. **129**, 090401 (2022).
[65] J. B. Kogut, Rev. Mod. Phys. **51**, 659 (1979).
[66] A. Y. Kitaev, Ann. Phys. **303**, 2 (2003).
[67] A. Kitaev and C. Laumann, in *Exact Methods in Low-dimensional Statistical Physics and Quantum Computing*, Lecture Notes of the Les Houches Summer School No. 89 (Oxford University Press, 2010) Chap. 4, pp. 101–125.
[68] L. Savary and L. Balents, Phys. Rev. Lett. **108**, 037202 (2012).
[69] S. Lee, S. Onoda, and L. Balents, Phys. Rev. B **86**, 104412 (2012).
[70] R. Moessner, S. L. Sondhi, and P. Chandra, Phys. Rev. B **64**, 144416 (2001).
[71] R. Zitko, Comput. Phys. Commun. **182**, 2259 (2011).
[72] M. P. A. Fisher, "Duality in low dimensional quantum field theories," in *Strong interactions in low dimensions*, edited by D. Baeriswyl and L. Degiorgi (Springer Netherlands, Dordrecht, 2004) pp. 419–438.
[73] E. Fradkin, *Field Theories of Condensed Matter Physics*, 2nd ed. (Cambridge University Press, 2013).
[74] E. Fradkin and L. Susskind, Phys. Rev. D **17**, 2637 (1978).
[75] E. Fradkin, M. Srednicki, and L. Susskind, Phys. Rev. D **21**, 2885 (1980).
[76] M. Žukovič, Phys. Lett. A **404**, 127405 (2021).
[77] R. Moessner, S. L. Sondhi, and P. Chandra, Phys. Rev. Lett. **84**, 4457 (2000).
[78] Y. Huh, L. Fritz, and S. Sachdev, Phys. Rev. B **81**, 144432 (2010).
[79] Y. Huh, M. Punk, and S. Sachdev, Phys. Rev. B **84**, 094419 (2011).
[80] R. Moessner and S. L. Sondhi, Phys. Rev. B **63**, 224401 (2001).
[81] F. Yang and H. Yao, Phys. Rev. Lett. **109**, 147209 (2012).